NUMERICAL MODELLING OF FLUID FLOW AND HEAT TRANSFER IN A DUAL-POROSITY DOMAIN IN THE SHALLOW ZONE OF THE NESJAVELLIR GEOTHERMAL SYSTEM

Esteban Gómez-Diaz[1]*, Juliet Newson[2], Samuel Scott[2,3], Thomas Ratouis[4],

[1]Energy and Minerals Resources Group, RWTH Aachen University, Wüllnerstraße, 52056 Aachen, Germany

[2] Iceland School of Energy, Reykjavik University, Menntavegur 1, 102 Reykjavik, Iceland

[3]University of Iceland, Sæmundargata 2, 102 Reykjavik, Iceland

[4]Carbfix, Bæjarháls 1, 110 Reykjavík, Iceland.

e.gomez@geol.rwth-aachen.de

Keywords: Numerical modelling, *Dual porosity, MINC, Geothermal reinjection.*

ABSTRACT

A numerical model of the warm wastewater re-injection zone was developed for the Nesjavellir geothermal field in Iceland. A detailed shallow 3D geological model was built to constrain the numerical model, with a dual-porosity based on Multiple Interactive Continuum (MINC) was considered as fracture model. The calibration method used was underground water temperature data measured between 1998 - 2019, along with tracer test data carried out in the area between 2018 - 2019. The temperature simulation showed acceptable results matching with the temperature field, and the tracer model closely matches the overall tracer return in the most of the monitoring stations. With the model calibrated we proceeded to simulate two future scenarios for a period of 20 years. The first scenario assumes that the injection continues, and in the second scenario the injection is completely stopped. The numerical model in this study allowed a better characterization of the fracture matrix interface and the porosity of postglacial lava flows, along with a clearer understanding of the connections between injection wells and monitoring stations, providing solutions for sustainable management of the geothermal resource and the surrounding environment.

1. INTRODUCTION

1.1 Nesjavellir Geothermal Field

The Nesjavellir Geothermal Field is a high-enthalpy geothermal system in southwest Iceland situated in a rift valley, extending from north of Hengill region to Lake Thingvellir about 25 kilometers east of Reykjavik in the Western Volcanic Zone (Figure 1). There, the Nesjavellir power plant operates with a combined cycle plant, wherein a mixture of steam and geothermal brine is transported from the wells to a central separation station at 200 °C and 14 bars, generating 120 MW of electricity and 290 MW as district heating supply to Reykjavik. Excess water from the separated liquid and condensed steam is dumped into shallow reinjection wells near the power plant or into a nearby surface stream. Warm water percolates below in both circumstances, raising groundwater temperatures. As a result this warm water discharged from the outflow connecting to Lake Thingvellir is a potential enviroment risk. Because of that, a monitoring effort involving tracer testing was carried out to acquire a better understanding of subsurface fluid flow routes in order to better understand and minimize this problem. This temperature and tracer data, along with geology data, is utilized to calibrate the numerical model provided in this paper.

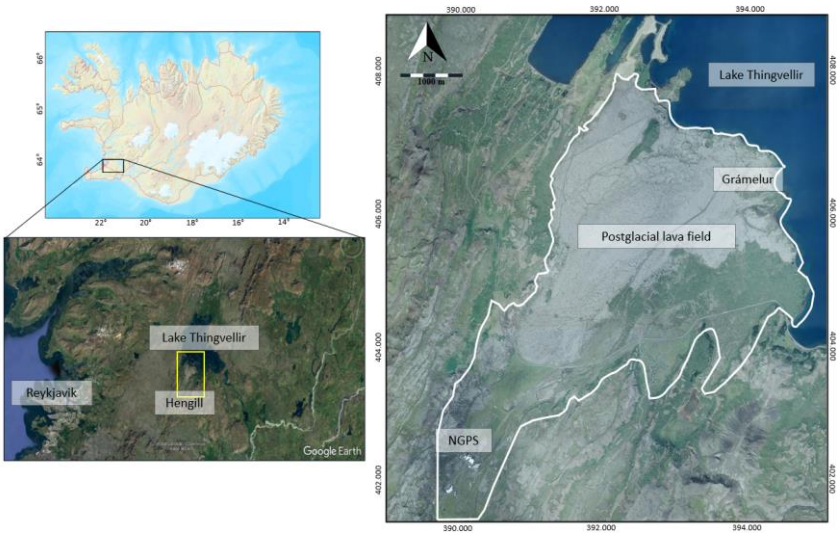

Figure 1: Location of Nesjavellir geothermal field. Yellow box is the study zone, and the main area of interest is within the white border line. NGPS: Nesjavellir Geothermal Power Station.

ISSN 2703-4275

1.2 Surface Geology

The geothermal field is a high-enthalpy geothermal system related to the one of the largest high temperature areas of the country, where the geothermal activity is closely connected to three active volcanic systems. The area is almost entirely built up of volcanic rocks of late Quaternary and postglacial age (Arnason et al., 1969), consisting mainly of hyaloclastite formations erupted during glacial periods and lava flows erupted during interglacial periods. Intrusions dominate at depths >1 km, and intermediate and felsic rocks are found at depth in many drill holes in the field (Franzson 1988; Franzson et al., 2010). Two significant fault sets are associated with a 10-kilometer-wide graben structure that runs NE-SW, parallel to the hyaloclastite ridges (Franzson, 1988). The NE-SW graben has one fault system that runs parallel to it. The other system is oblique to the graben structure, with a strike that cuts down the valley from north to south (Franzson, 1988). The N-S trending faults appear to act as partial barriers to northeastward flow over the NE-SW structures (Figure 2), and the geothermal system is mostly insulated from the upper groundwater layers by a low permeability cap rock layer at roughly -600 masl..

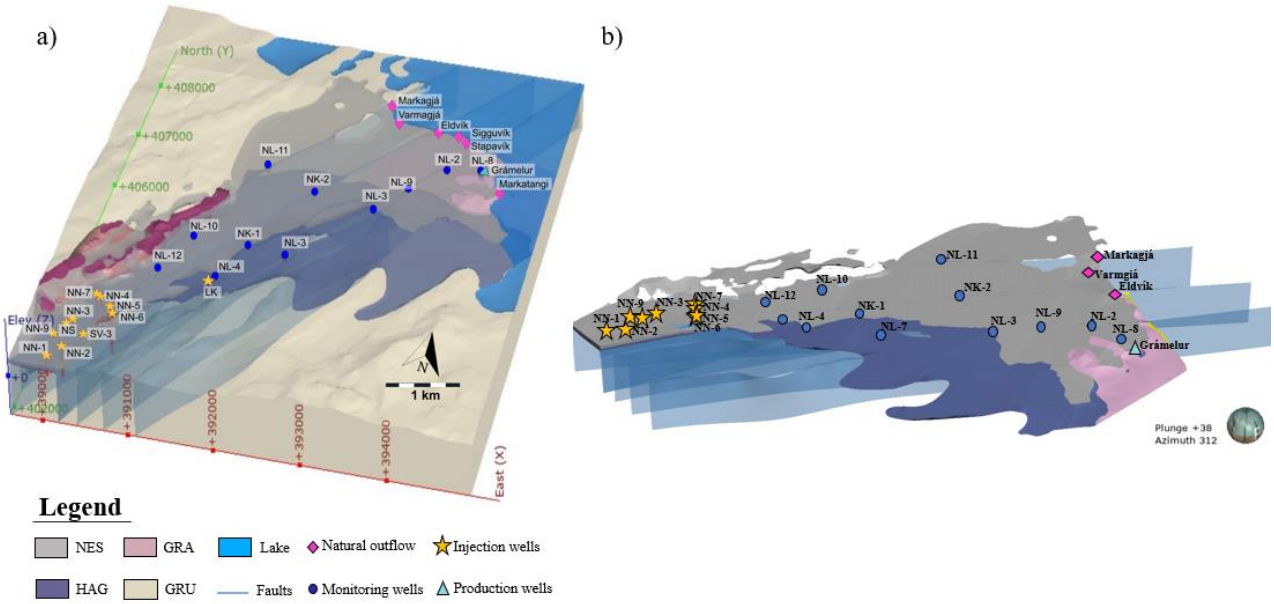

Figure 2: a) 3-D geological model with fault planes projection. b) Detailed view of lava flows and fault planes.

1.3 Wastewater Disposal and monitoring in Nesjavellir

Most of the condensate water has been dumped into a shallow well near the power station when the Nesjavellir geothermal power plant began generating energy in 1990 utilizing four wells, and the separated water was discharged into a surface stream somewhat farther upstream. More wells were needed to compensate for the increased hot water production as the geothermal plant expanded its output and hence more wells were utilized. In 1997, a 25-meter-deep well (SV-3) was drilled near the current cooling tower. Since then, excess hot water has been fed into this shallow well. When SV-3 overflows (at 400 to 500 l/s), the extra water is discharged into the surface stream. After a reinjection campaign was started in 2004, almost all the separated water was injected in the higher levels of groundwater, and excess separated water was diverted to the stream. In 2020, nine shallow reinjection wells were in use with around 250 – 300 l/s of separated water and 100 – 150 l/s of condensate water going into the reinjection wells.

Tracer tests and other subsurface experiments have been used to explore the subsurface flow of geothermal water through shallow lavas in the Nesjavellir area. The geothermal water has been traced from Lækjarhvar (LK) to various lakeshore springs using a sodium fluorescein tracer (Kjaran and Egilsson, 1986, 1987). The flow showed to be confined to a very narrow area between Markagjá in the north and Stapavik in the south, with the core of the flow located upwards of the Varmagjá area (Kjaran and Egilsson, 1986, 1987; Ólafsson, 1992). Temperature profiles from experimental drillholes in Nesjahraun showed that the flow of the geothermal water is also confined vertically to a narrow zone a few meters above the cooler ground water table (Wetang'ula, 2004). Since 2000 Iceland Geosurvey (ISOR) has been monitoring excess water flow of the power plant. The monitoring consists of annual groundwater temperature logging in wells NK-1, NK-2, NL-2, NL-3, NL-4, NL-7, NL-8, NL-9, NL-10, NL-11 and NL-12. Data has been visualized with a 2D map showing temperature isotherms at 1 m depth below the groundwater table (Hafstað, 2000a, b, c, 2001a, b, 2003, 2006; Hafstað and Kristjánsson, 2006; Hafstað et al., 2007; Þorbjörnsson et al., 2009; Kristinsson and Hafstað, 2011; Kristinsson and Níelsson, 2012; Hafstað and Níelsson, 2013; Hafstað, 2014; Ingimarsson and Hafstað, 2015; Ingimarsson et al, 2016; Čypaitė and Ingimarsson, 2017, Čypaitė, 2018). Figure 3 shows the temperature at 1 meter below of the of the ground water in 2019 along with the distribution of injection, production, monitoring wells, and springs with an illustration of the feedzones.

ISSN 2703-4275

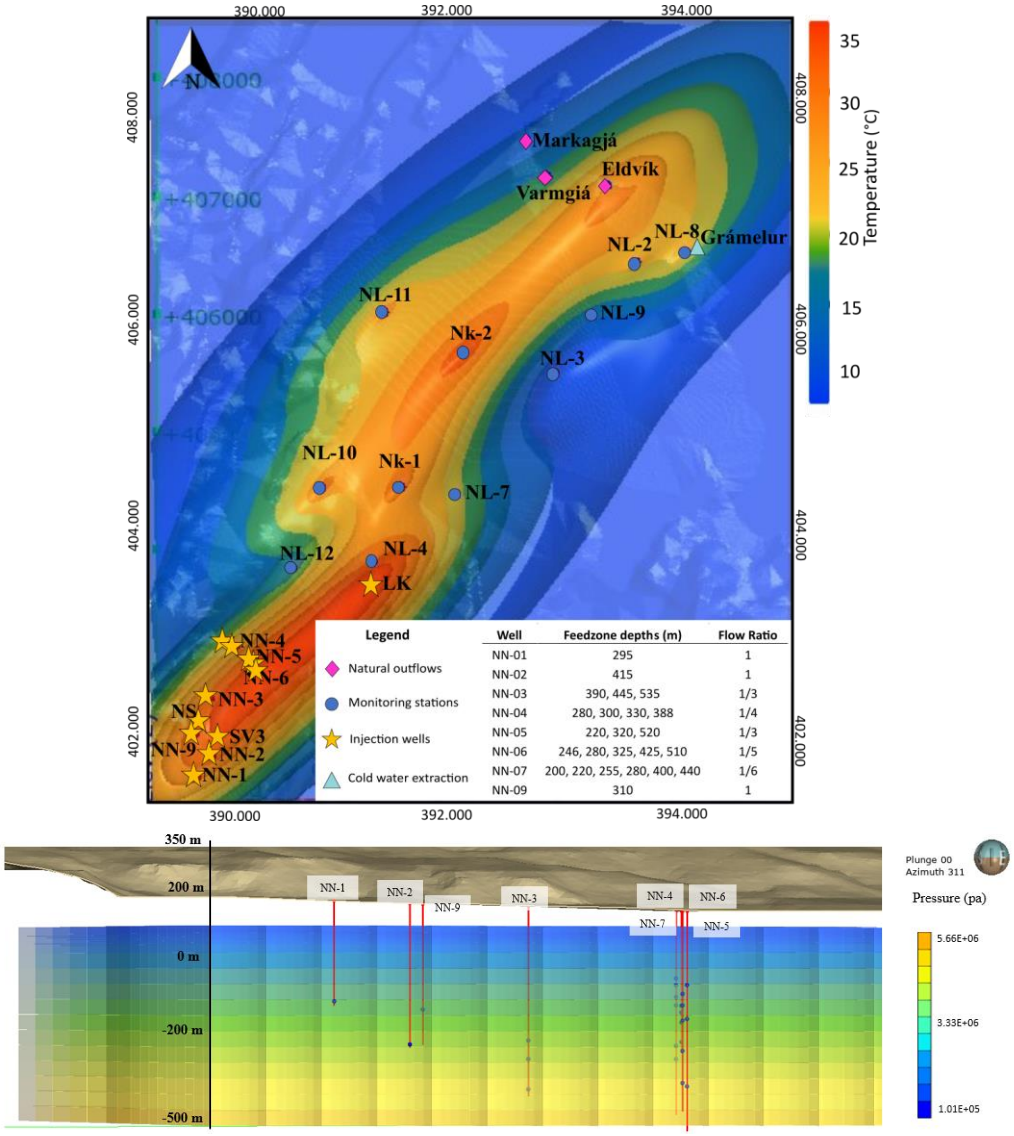

Figure 3: Map view of the temperature model at one meter from the ground water in 2019. The map shows the distribution of injection, production, monitoring wells, and springs used considered in the study. The lower chart illustrates the feedzones (blue spheres) and injection wells (red spheres). Its transparent colors indicate the initial pressure distribution in the model around the injection zone.

2. METHODOLOGY

2.1 Model set-up

The TOUGH2 (Pruess et al., 1999) simulator was used to perform numerical simulations of shallow reinjection and tracer transport. The numerical technique employed in TOUGH2 is briefly described below, with an emphasis on the model setup as well as the tracer and temperature data needed to calibrate the numerical model. Fluid properties are calculated using equation-of-state module EOS1, which means fluid in the numerical model is assumed to be pure water with properties given by IAPWS-95 (Wagner and Pruß, 2002). The EOS1 module is suitable to simulate tracer transport with AUTOUGH2 (Yeh et al., 2012). The model was set-up as a dual-porosity model based on the Multiple Interacting Continua (MINC) (Pruess and Narasimhan, 1985; Pruess, 1992) approach. The dual-porosity model of Nesjavellir used three interacting continua (one fracture and two matrix blocks) with corresponding volume fractions of 10% - 20% - 70% and a fracture spacing of 100 m. The fracture was assigned a very high porosity fixed at 90%. The initial matrix porosity was chosen such that effective porosity of the dual-porosity model is the same as the porosity of the single porosity model. The MINC grid was applied only to the grid blocks within the central area limited by faults.

Leapfrog Geothermal was used to set up the conceptual model and the grid, and subsequently PyTOUGH (Croucher, 2011) was used to modify the grid and optimize it in the reinjection area (Figure 4). The model has a total surface area of 7880 m2 and 618 m thickness. Reykjavik Energy provided the groundwater table data that defined the top surface. The range of depth is 19.69 masl to -500 masl to reflect the shallow flow more precisely, with 19 layers of 45 m thickness and two thinner near-surface layers of 5 m and 20 m thickness. A 31° rotation of the grid was performed with the intent of having the grid parallel to the rift and some of the major NNE-SSW faults. The model can use fault-parallel permeability that is higher than horizontal permeability perpendicular to the fault

ISSN 2703-4275

since the grid is aligned with the structure. 22133 elements make up the mesh. TIM (Yeh et al., 2013) and Leapfrog Geothermal were used to visualize the grid and model findings, respectively.

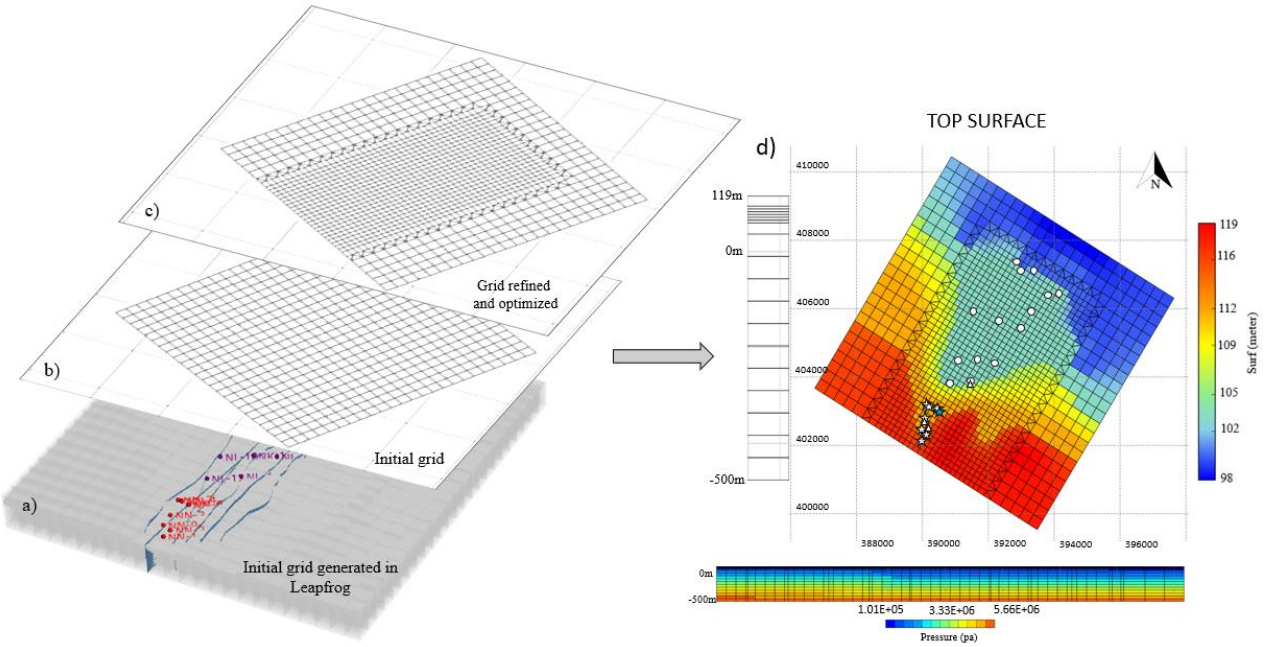

Figure 4: a) Grid generated with Leapfrog program. b) Grid visualization in TIM. c) Grid refined and optimized with PyTOUGH. d) Final grid with the conceptual model visualized in TIM.

Previous modeling studies of the Hengill area (Bodvarsson et al., 1990; Zakharova and Spichak, 2012; and Snbjörnsdóttir et al., 2014; Gunnarsson & Aradóttir, 2014) were used to develop the hydrological parameters for the main rock types. CHN10, CHN20, CHN30, and FEED0 were introduced to the conceptual model as high permeability rocks. The rock types CHN10, CHN20, and CHN30 correspond to permeability channels over the lava field, as indicated primarily by the monitoring recovery curve and temperature rising trend from field data. The upper half of the layer that limits the flow between groundwater and the geothermal system is known as the bottom boundary (BOUN0). The injected water follows for the upper groundwater zone are constrained to a narrow SW-NE trending zone contained by lower permeability rocks on the NW and SE borders, and below roughly 50 m depth, according to the conceptual model and tracer test. These low permeability zones extend to the boundaries of the numerical model. Table 1 shows the calibrated permeability values for the initial and additional rock types. Constant atmospheric conditions are applied over most of the top surface of the model, with a fixed pressure of 101325 Pa and temperature of 10 °C. For the columns lying under the lake (WETB0), a hydrostatic pressure corresponding to the depth of the lake and a constant temperature of 10 °C were assigned as a top boundary condition. The bathymetry of the lake was retrieved from Stevenson et al. (2011). Figure 5 shows the calibrated model structure on the top surface and cross-sections.

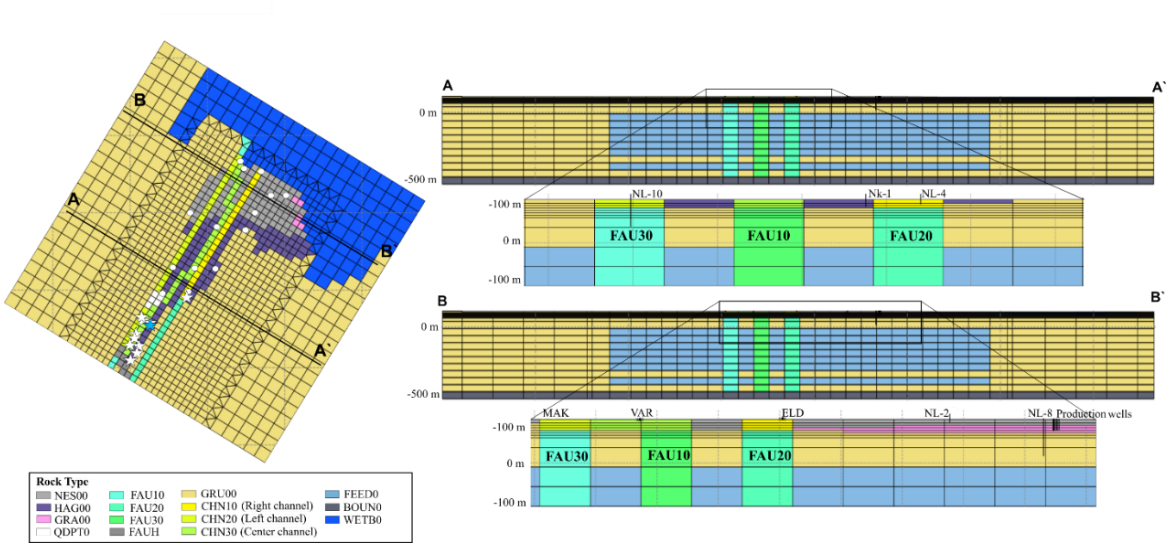

Figure 5: Calibrated model structure, top surface. White stars are injection wells, blue star NN-6 well and white points are monitoring points.

ISSN 2703-4275

Table 1: Calibrated permeability values for each rock type.

ROCK TYPE	Permeability		
	kx (m^2)	ky (m^2)	kz (m^2)
GRA0	$1e10^{-09}$	$1e10^{-09}$	$1e10^{-11}$
GRU0	$1e10^{-14}$	$1e10^{-14}$	$1e10^{-15}$
HAG0	$1e10^{-09}$	$1e10^{-09}$	$1e10^{-15}$
NES0	$1e10^{-09}$	$1e10^{-09}$	$1e10^{-15}$
FAUH0	$1e10^{-16}$	$1e10^{-16}$	$1e10^{-16}$
FAU10	$3e10^{-11}$	$5e10^{-10}$	$5e10^{-13}$
FAU20	$3e10^{-12}$	$5e10^{-11}$	$5e10^{-13}$
FAU30	$3e10^{-12}$	$5e10^{-12}$	$5e10^{-13}$
BOUN0	$1e10^{-16}$	$1e10^{-16}$	$1e10^{-16}$
CHN10	$9e10^{-09}$	$9e10^{-09}$	$1e10^{-15}$
CHN20	$8e10^{-09}$	$8e10^{-09}$	$1e10^{-15}$
CHN30	$9e10^{-09}$	$9e10^{-09}$	$1e10^{-15}$
FEED0	$1e10^{-11}$	$1e10^{-11}$	$5e10^{-14}$
QDTP0	$1e10^{-16}$	$1e10^{-16}$	$5e10^{-16}$

2.2 Calibration

The model was manually calibrated to generate a return profile that is in good agreement with the measured tracer and temperature data. Despite the fact that the models replicate the system over separate time periods, the tracer and temperature data were calibrated together because both models are sensitive to geologic structure and rock qualities (mainly permeability). Internal reports by Reykjavik Energy and ISOR provided the temperature data utilized for the calibration. Reykjavik Energy has been monitoring the natural discharges Lækjarhvar, Varmagjá, Sigguvík, Markagjá, Markatangi, Eldvík and Gramelur since the early 2000s. Meanwhile, since the early 2000s, ISO has maintained an annual record of groundwater temperature in wells NK-1, NK-2, NL-2, NL-3, NL-4, NL-7, NL-8, NL-9, NL-10, NL-11, and NL-12 using data from monitoring stations.

The tracer tests used to calibrate the simulation model involved the injection of 2,7-NDS (Naphthalenedisulfonic acid disodium salt) in NN-6 well during November 2018 to September 2019. The injection rate was 115 L/s on average, with 100 kg of tracer material injected. Recovery was seen in the NK-1, NK-2, NL-4, and NL-12 wells 30 days after the injection, with the highest concentration peaks in the NK-1 and NK-2 wells. Natural outflows and NL-2 have a second recovery period of 70-80 days, with a third arrival possible after 150 days. The location of injection wells and monitoring points and tracer recovery is illustrated in Fig. 6, where the recovery data will be used to calibrate the simulation model.

From January 1, 1998, until November 5, 2018, a single water component is used in the temperature simulation. This model incorporates the above-mentioned beginning circumstances, as well as injection and production data for all wells, as well as a reinterpretation of the structures based on the 2018 to 2019 tracer recovery test. The tracer calibration is a two-part simulation that simulates the injection of the tracer into the proper model wells. From the 15th of November 2018 to midnight on the 20th of September 2019, the model simulates tracer advection. During this simulation, the geothermal fluid injection and monitoring wells remain in the other wells in the system. During the simulation, a small amount of tracer (1x10-10 kg tracer per kg injected water) was co-injected within the injection wells NN-01, NN-02, NN-03, NN-04, NN-06, NN-07, NN-09 and surface injection point Lk to keep the steady tracer background value constant and prevent heavy dilution in all injection elements.

3. RESULTS AND DISCSUSION

3.1. Temperature model

The simulation matches the monitoring well temperature data quite well over time, reproducing the general rate and amount of temperature increase. For NK-01, NK-02, NL-10, and NL-04, the best matches were found, see figure 6. The varied infusion of hot water (changing mass or changing temperature) over different time periods causes seasonal changes in the order of 10 °C. Wells NL-02, NL-07, NL-08, and NL-09 exhibited modest findings, but NL-11 revealed temperatures that were much lower than field data. According to field data, the temperature increase in natural outflows is lower than in shallow monitoring wells (Figure 6). Eldvik reproduces the seasonal effect but predicts a smaller size than what has been observed. While Markagjá experienced a minor increase in the early 2000s, the curve began to decline once the well was injected. Despite the fact that data suggest Varmagjá will see the biggest temperature increase, models forecast a similar magnitude of increase as the other natural outflows, resulting in a 10 to 13 °C difference between the model and the field data.

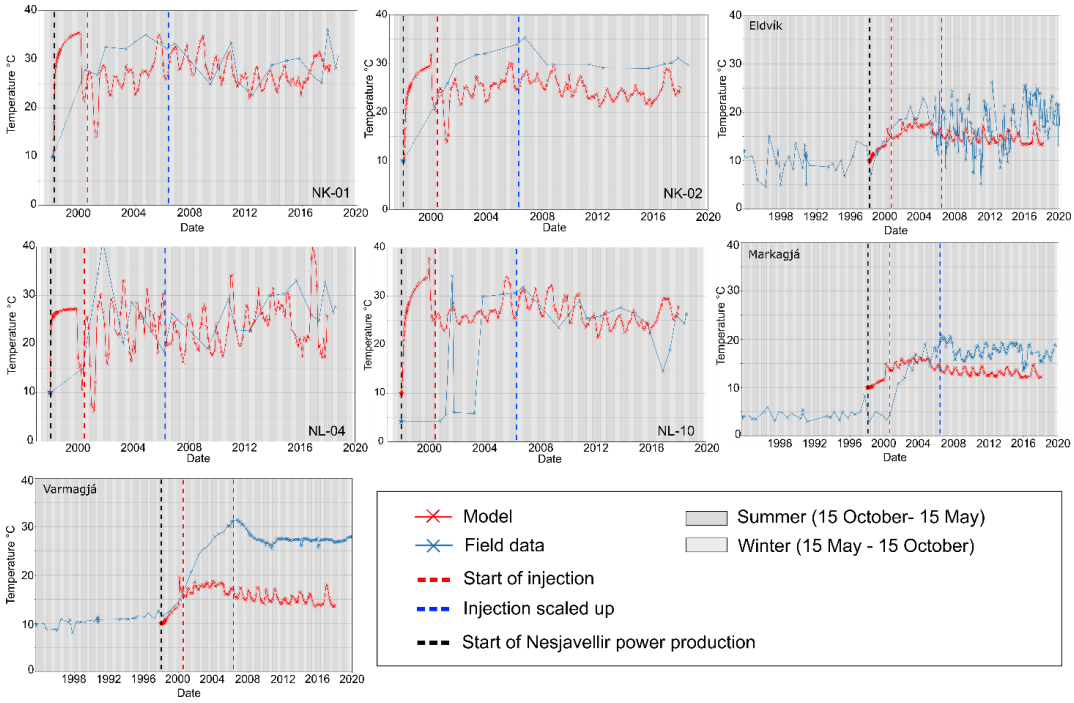

Figure 6: Evolution of temperature from 1998 to 2018 at one meter of groundwater level (layer 1) in NK-01, NK-02, NL-04 and NL-10 and outflows. Field data in blue and model results in red.

The presence of shallow high permeability aquifers near the surface, as well as significant rift-parallel faults, which transfer heat from reinjection to the NW along the rift, govern heat transport. The temperature distribution in the lava field at 100 masl (layer 1) is compared to ISOR interpreted isotherms for September 2000, October 2006, and May 2017. A plume with temperatures of 20-40 °C forms roughly centered along the most permeable fault shortly after the start of shallow reinjection (Figure 7). Temperatures along the fault (FAU10) reveals that only the uppermost high permeability lava field are hotter. Because of the infusion of warm water at deep levels has not yet begun, the temperature at higher depths remains unaltered. The simulation shows that temperature rises fastest in the NE-SW direction, reaching 30 °C in the center of the field and 15 to 20 °C near the lake, which is a good match to the field data. Furthermore, the models replicate the bending of the thermal plume towards the west along Lake Thingvellir's shore. Temperatures had risen to around 20 °C across most of the lava field by October 2006 (Figure 7b), with the area between 20 °C and 30 °C isotherms extending to the lake. The simulation indicates a low temperature zone (15 °C) between NK-02 and NL-11, which is expected because this area is not in the high permeability zone and, while it might be influenced by faults as well, it was decided to segregate it owing to a lack of data. Temperatures around the deep injection wells (NN-3, NN-4, and NN-5) have grown to 60 °C at depths 0 to 500 m, but reach a shorter distance to the NW than temperatures in the shallow lava flow. Temperatures have risen to 35 °C in the center of the area by May 2017 (Figure 7c), especially along the injection well to NK-02 and along the lake's margin. However, temperatures have risen over a large portion of the lava field, with a northeast trend evident in both field data and computer simulation results. The temperature has risen dramatically at deeper levels, even reaching a shallow level below NK-01 and NK-02. Over a vast vertical region in the subsurface, the temperature is roughly 30 - 40 °C and extends 3-4 km to the NW along the main rift-parallel fault. The bend in the thermal plume to the west in the vicinity of Lake Thingvellir is clearly visible, although the model predicts somewhat high temperatures (~20 °C) extend 1 km to the SW.

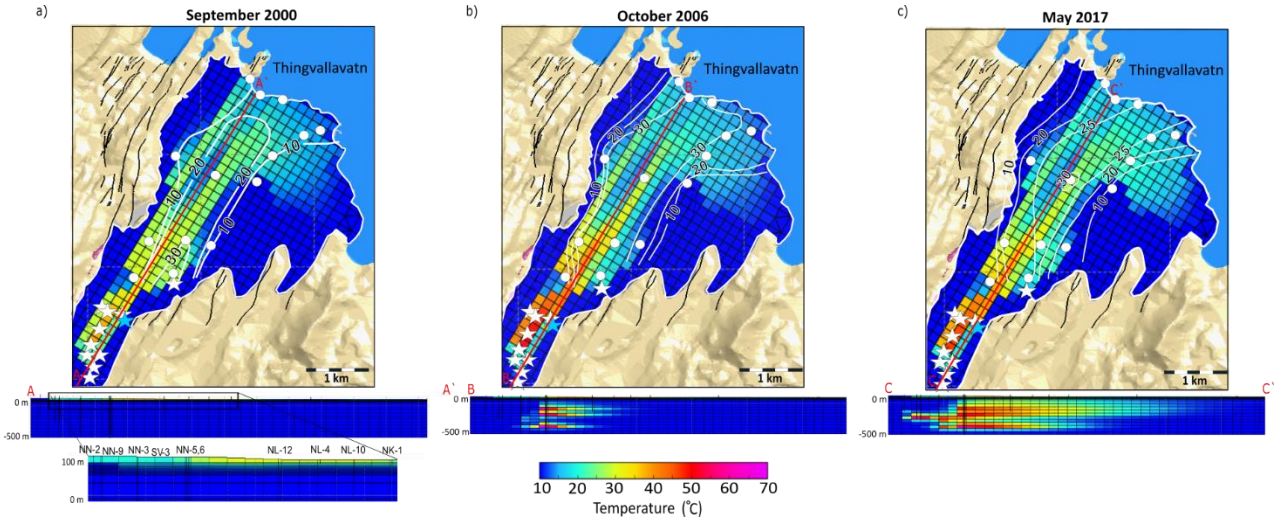

Figure 7: a) Comparison between temperature ISOR map with simulation results for September 2000, October 2006, and May 2017 at temperature one meter the below groundwater table b) Cross section along the most permeable fault (FAU10).

3.2. Tracer model

The single porosity model shows poor results in terms of matching the tracer recovery curves. The tracers appear only in NK-1, NK-2 and NL-4, and neither arrival time nor recovery concentration match those observed in the field showing the limitation based on this model and supporting the feasibility of using dual porosity model. The dual porosity model shows a shallow high permeability lava flow at shallow depths and the SW-NE directed fault at higher depths restricts tracer advection. The model results are in good accord with the field data gathered during the 2018-2019 tracer test. The tracer comparison distribution for single and dual porosities at 86 masl and -180 masl are visualized in Figure 8 and dual porosity tracer recovery curves are shown in the Figure 9. Within the shallow lava flow, there is a relatively broad (0.5 km) plume of tracer. This plume drifts to the northwest and reaches the shores of Lake Thingvellir after 84 days. The highest tracer concentrations in the shallow lava flow are localized in a small area around the lake after 126 days. Tracer concentrations are much higher at greater depth along the main NW-SE-oriented fault. While the tracer mass at depth within the fault is greater than the shallow lava flow, the anomaly is not as large.

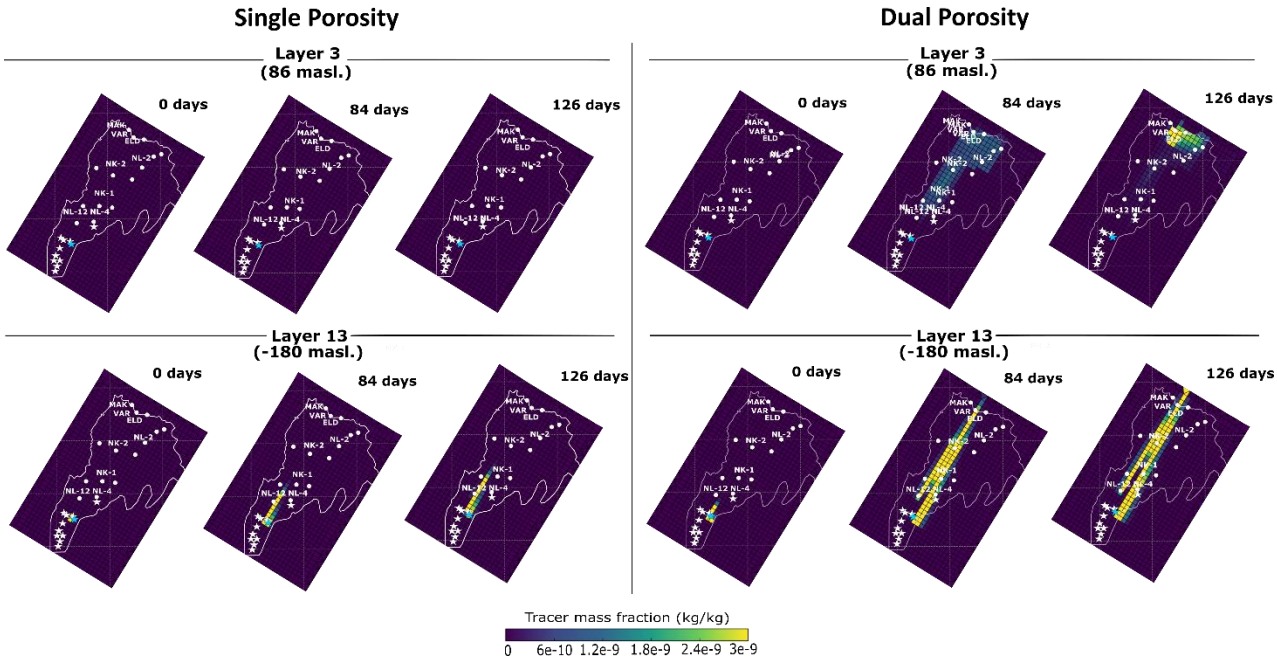

Figure 8: Single porosity model results (left) and dual-porosity model results (right). Tracer content in 2018 to 2019 at an elevation of 86.2 masl (layer 3) and -180 masl (layer 13).

In several of the monitoring stations, particularly NK-01 and NK-02 (Fig. 9a,b), the simulations reproduce the overall arrival time, peak tracer concentration, and form of the measured tracer return curves. In comparison to simulations, field data show a faster tracer return in the natural outflows of Eldvik, Markagjá, Varmagjá, (Fig. 9c-e). The predicted and measured tracer concentration peaks in

wells NL-02 (Fig. 9f) suggest a broader peak than the tight peak reported in the field and a constant arrival but close to the highest peaks seen on field for NL-04 (Fig. 9h). The simulations show no tracer arrival for NL-12 (Fig. 9g), although very low concentrations were measured.

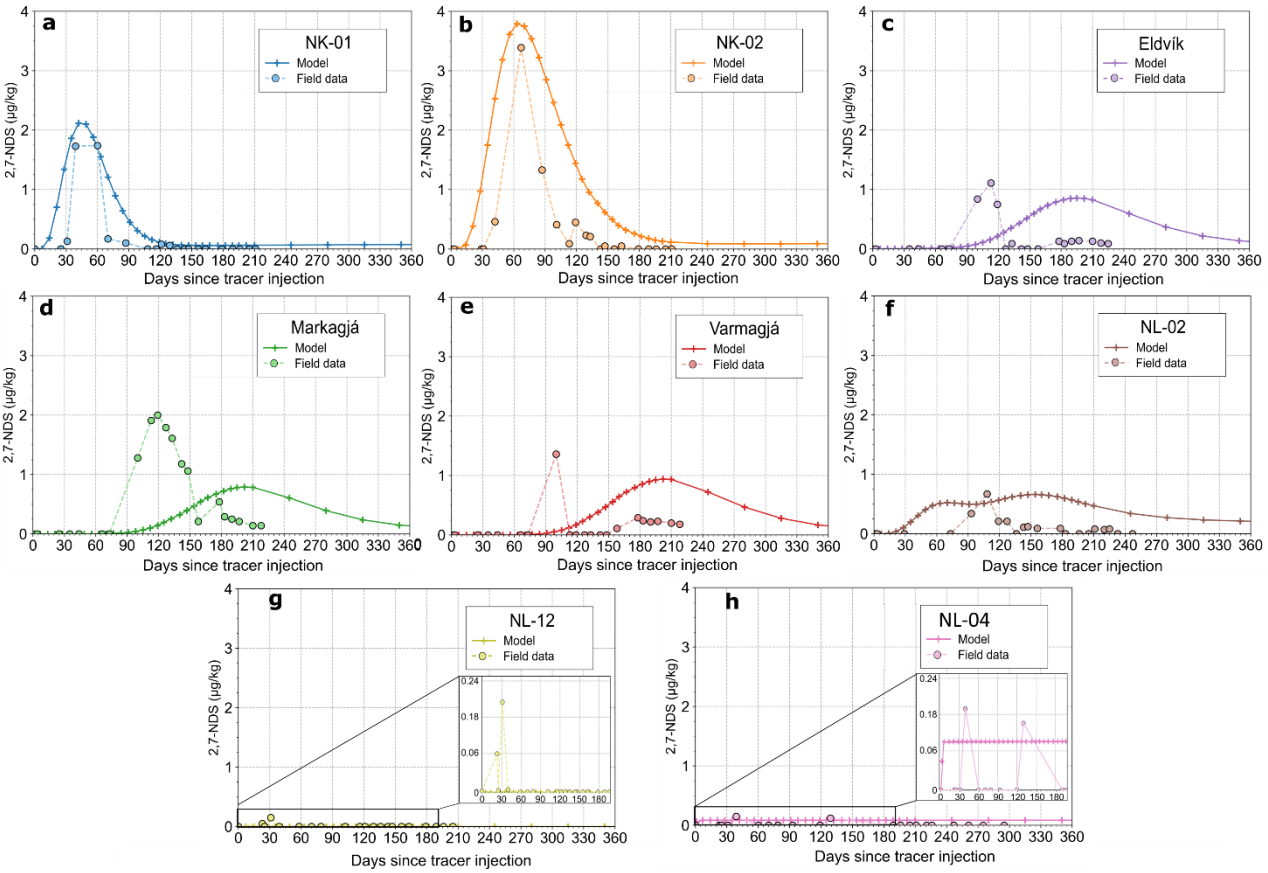

Figure 9: Dual-porosity model results - Tracer recovery curves for 2,7-NDS tracer injection (µg/kg). The field data is represented by the dots and the dotted line, and the model results by the plus sign symbol and the solid line.

3.3. Forecast out to 10 and 20 years

The calibrated model was used to analyse two different future scenarios. In the first, the injection is continued for another 20 years at the same rate and temperature as in 2018-2019. All shallow and deep reinjection, on the other hand, is halted across the field. Figure 10 depicts the temperature distribution over 10 and 20 years at one meter below the water table, at 86 masl and -180 masl, respectively. Temperatures near the surface increase very little along the lake's border after ten years of reinjection, but temperature rises were more pronounced at deep along the main rift parallel fault, with temperature increases of up to 45 °C and 60 °C at 86 masl and -180 masl, respectively. Most of the shallow lava field had temperatures above 25 °C after 20 years, with temperatures nearing 35 – 40 °C in the main channels and 30 °C near the lake. The maximum temperature at 86 masl is around 60 °C, with temperatures in the main channel around 50 °C and in the Grámelur area around 40 °C. The zone of elevated temperature (60 °C) reaches the shoreline at depths of -180 masl. The increasing temperatures along the most permeable fault are highlighted by vertical cross sections in Figure 9. In the second scenario the injection and production in the field were stopped. In this case, after fewer than two years, the temperature lowers dramatically on the surface, but more slowly at depth. After ten years, the shallow temperature is 12 -13 °C, which is similar to the starting temperature before reinjection. Temperatures above 30 °C persist at higher depths in the area surrounding the injection zone and along the main channel, although the area closer to the lake cools quickly.

ISSN 2703-4275

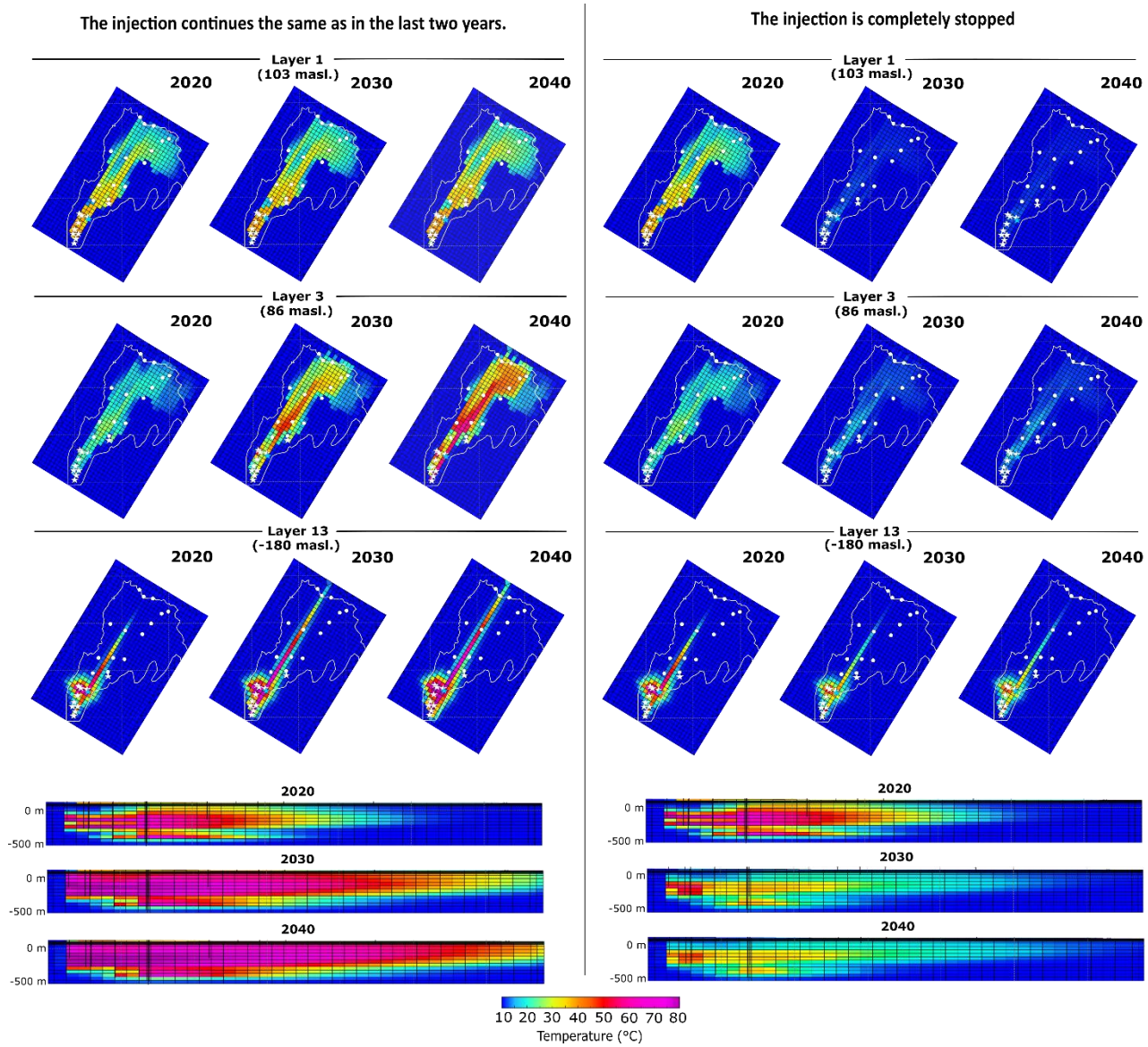

Figure 10: Evolution of temperature in 2020, 2030 and 2040 if injection and production continue at the same average flow rate and temperature from 2018 – 2020 (left), and all injection and production is stopped (right). Cross sections along the most permeable fault (FAU10) are shown below.

4. CONCLUSION

The use of a dual porosity, Multiple Interacting Continua (MINC) approach to enhance the resolution of spatial discretization in the narrow flow channel showed better matches to data than a single porosity approach, as would be expected for a fracture- permeability dominated system such as Nesjavellir. A dual-porosity approach reduces the effective volume of the block that the fluid flows through (fractures), causing the tracer travel time between the injection well and the production wells to be significantly faster. Two main permeable channels were defined, where the flow is largely confined within these permeable features found between the reinjection zone to the lake. The measured tracer recovery and peak for the monitoring stations fits well with the simulations, but the tracer arrival time for natural outflows could be improved. The medium appears to be substantially anisotropic at deep depths, with large faults acting as a preferred conduit for re-injected fluid. Fluid easily flows through the fault zone where fractures connect with shallow permeable channels at shallow levels, allowing some of it to reach the surface layers. However, the area around the lake has complex technical characteristics, and the transport mechanism of fluid in that area is relatively unknown. In response to reinjection, the numerical model reproduces rising temperatures within the postglacial lava flow. For most monitoring stations, the model demonstrates a satisfactory fit, which reflects a depiction of the temperature spread from 1998 to 2018. Between the Nesjavellir reinjection zone and Lake Thingvellir, there are two main permeable channels, and flow is generally limited within these permeable features. The measured tracer recovery and peak for monitoring stations match the calculations well, but the tracer arrival time for natural outflows might be faster.

The model indicates that it is possible to forecast the system's likely behavior if the temperature and tracer simulations match the field data with the set hydrological parameters. With continual injection, the temperature will be around 35 °C for shallow levels (-90

masl) and higher than 50 °C for intermediate and deeper depths below the Lake Thingvellir lava flow limit after 20 years. After only a few years, the temperature over the entire lava flow field, especially around Lake Thingvellir, will be close to initial condition shallow levels if the injection is interrupted and not resumed. According to the model, the area around the deepest injection zone will take more than 20 years to settle down to near steady state temperature.

ACKNOWLEDGEMENTS

The authors thank Reykjavik Energy for providing valuable data, assistance, and support during this research.

REFERENCES

Arnason, B., Theodorsson, P., Bjornsson, S., and Saemundsson, K., 1969. Hengill, a high temperature thermal area in Iceland. Bull. Volcanol., 33, 245-259.

Bodvarsson, G.S., Bjornsson, S., Gunnarsson, A., Gunnlaugsson, E., Sigurdsson, O., Stefansson, V. and Steingrimsson, B. 1990. The Nesjavellir Geothermal Field, Iceland, Part I. Field Characteristics and Development of a Three-dimensional Numerical Model. Geothermal Science and Technology, 2(3): 189-228.

Croucher, A. 2011. PyTOUGH: a Python scripting library for automating TOUGH2 simulations. In Proceedings: 33rd New Zealand Geothermal Workshop, Auckland, New Zealand.

Čypaitė, V. and Ingimarsson, H. (2017). Nesjavallavirkjun. Groundwater Temperature Measurements in 2017. Iceland GeoSurvey, ÍSOR-17160.

Čypaitė, V. (2018). Effluent Flow from Nesjavellir Power Plant. Iceland GeoSurvey, ÍSOR-2018/039.

Franzson, H. 1988. Nesjavellir-Borholujarðfræði, vatnsgengd í jarðhitageymi. OS-88046/JHD-09, 58 p.

Franzson, H., Gunnlaugsson, E., Árnason, K., Sæmundsson, K., Steingrímsson, B., and Harðarson, B.S., 2010. The Hengill Geothermal System, Conceptual Model and Thermal Evolution. In Proceedings: World Geothermal Congress 2010, Bali – Indonesia.

Gunnarsson, G. and Aradóttir E.S., 2014. The Deep Roots of Geothermal Systems in Volcanic Areas: Boundary Conditions and Heat Sources in Reservoir Modeling. Transport in Porous Media, vol. 108 (1), pp. 43–59.

Hafstað, Þ. H. (2000a). Nesjavellir. Mælingar í eftirlitsholum í Nesjahrauni. Orkustofnun, short report, ÞHH-2000-06. 10 p.

Hafstað, Þ. H. (2000b). Nesjavellir. Um eftirlitsholu norðan við orkuverið. Orkustofnun, short report, ÞHH-2000-18. 2 p.

Hafstað, Þ. H. (2000c). Nesjavellir. Boranir á afrennslissvæði. Staðan um aldamót. Orku-stofnun, short report, ÞHH-2000-22. 4 p.

Hafstað, Þ. H. (2001a). Nesjavellir. Hitamælingar á afrennslissvæði. Orkustofnun, short report, ÞHH-2001-13. 4 p.

Hafstað, Þ. H. (2001b). Nesjavellir. Um affallið í hrauninu. Orkustofnun, short report, ÞHH-2001-19. 4 p.

Hafstað, Þ. H. (2003). Niðurrennslisholurnar NN-3 og NN-4 á Nesjavöllum. Iceland GeoSurvey, short report, ÍSOR-ÞHH-2003/068. 8 p.

Hafstað, Þ. H. (2006). Nesjavellir. Hitamælingar á afrennslissvæði. Samanburður við fyrri mælingar. Iceland GeoSurvey, memo march 23, 2007, 5 p.

Hafstað, Þ. H. (2014). Nesjavallavirkjun. Hitamælingar á affallssvæði í nóvember 2014. Iceland GeoSurvey, short report, ÍSOR-14072.

Hafstað, Þ. H. and Kristjánsson, B. R. (2006). Nesjavellir. Myndir af útbreiðslu volga vatnsins í Nesjahrauni. Iceland GeoSurvey, memo Dec. 11, 2006. 7 p.

Hafstað, Þ. H., Vilmundardóttir E. G. and Kristjánsson B. R. (2007). Nesjavellir. Rannsóknarborholur í hraununum á affallssvæði virkjunarinnar. Iceland GeoSurvey, ÍSOR-2007/058, 65 p.

Hafstað, Þ. H. and Níelsson S. (2013). Nesjavallavirkjun. Hitamælingar á affallssvæðinu í október 2013. Iceland GeoSurvey, short report, ÍSOR-13087. 26 p.

Ingimarsson, H. and Hafstað, Þ. H. (2015). Nesjavallavirkjun. Hitamælingar á affallssvæði í nóvember 2015. Iceland GeoSurvey, short report, ÍSOR-15064. 19 p.

Ingimarsson, H., Čypaitė, V. and Hafstað, Þ. H. (2016). Nesjavallavirkjun. Hitamælingar á affallssvæði í nóvember 2016. Iceland GeoSurvey, short report, ÍSOR-16064. 20 p.

Kjaran, S.P. and Egilson, D. (1986). Nesjavellir. Effect of run-off water from scheduled geothermal power plant on ground water reservoir at Grámelur (in Icelandic). – Vatnaskil Consulting Engineers, report 86-03.

Kjaran, S.P and Egilson, D. (1987). Simulation of groundwater at Nesjavellir, (in Icelandic). Vatnaskil Consulting Engineers, report.

Ólafsson, J. (1992). Chemical characteristics and trace elements of Thingvallavatn. In: Jónasson, P.M. (ed.), Ecology of oligotrophic, subarctic Thingvallavatn, Iceland. Oikos, 64, 151-161.

Pruess, K. and T. N. Narasimhan, (1985). A Practical Method for Modeling Fluid and Heat Flow in Fractured Porous Media, Society of Petroleum Engineers Journal, 25, (1) 14-26, February.

Pruess, K. (1992). Brief Guide to the MINC - Method for Modeling Flow and Transport in Fractured Media. May, 1992. Earth Sciences Division, Lawrence Berkeley National Laboratory. Berkeley CA USA . LBL-32195.

Pruess, K., Oldenburg, C.M., Moridis, G.J. (1999). TOUGH2 User's Guide Version 2. Earth Sciences Division, Lawrence Berkeley National Laboratory. Berkeley CA, USA . LBNL-43134.

Snæbjörnsdóttir, S., Wiese, F., Fridriksson, T., Ármansson, H., Einarsson, G. M., Gislason, S. R., 2014. CO2 storage potential of basaltic rocks in Iceland and the oceanic Ridges. Energy Procedia, 63, 4585–4600

Þorbjörnsson, D., Ólafsson, G. E. and Hafstað, Þ. H. (2009). Nesjavellir. Hitamælingar í eftirlitsholum á affallssvæði í maí 2009. Iceland GeoSurvey, short report, ÍSOR-09052. 20 p.

Wagner, W., Pruß, A., 2002. The IAPWS Formulation 1995 for the Thermodynamic Properties of Ordinary Water Substance for General and Scientific Use. J. Phys. Chem. Ref. Data, 31 (2), 387-535.

Wetang'ula, G., (2004). Assessment of geothermal waste water disposal effects, case studies:Nesjavellir (Iceland) and Olkaria (Kenya) fields. University of Iceland, MSc. thesis, UNU-GTP,Iceland, report 2, 76 pp.

Yeh, A., Croucher, A. and O'Sullivan, M.J., 2012. Recent developments in the AUTOUGH2 simulator. In Proceedings: TOUGH Symposium, Berkeley, California, September 17-19.

Yeh, A., Croucher, A. E., and O'Sullivan, M. J., 2013. TIM–Yet another Graphical Tool For TOUGH2. In Proceeding: 35th New Zealand Geothermal Workshop, Rotorua, New Zealand.

Zakharova, O. K., and Spichak, V.V., 2012. Geothermal fields of Hengill Volcano, Iceland. Journal of Volcanology and Seismology, vol. 6, no. 1, pp. 1–14

ISSN 2703-4275